Model-Based Adaptive Behavior Framework for Optimal Acoustic Communication and Sensing by Marine Robots

Model-based Adaptive Behavior Framework for Optimal Acoustic Communication and Sensing by Marine Robots

Toby Schneider, *Member, IEEE,* Henrik Schmidt

***Abstract*—A hybrid data- and model-based autonomous environmental adaptation framework is presented which allows autonomous underwater vehicles (AUVs) with acoustic sensors to follow a path which optimizes their ability to maintain connectivity with an acoustic contact for optimal sensing or communication. The adaptation framework is implemented within the behavior-based MOOS-IvP marine autonomy architecture and uses a new embedded high-fidelity acoustic modeling infrastructure, the Generic Robotic Acoustic Model (GRAM), to provide real-time estimates of the acoustic environment under changing environmental and situational scenarios. A set of behaviors that combine adaptation to the current acoustic environment with strategies that extend the decision horizon beyond that of typical behavior-based systems have been developed, implemented, and demonstrated in a series of field experiments and virtual experiments in a MOOS-IvP simulation.**

***Index Terms*—Underwater technology, Underwater acoustics, Robot sensing systems**

I. Introduction

Autonomous underwater vehicles (AUVs) are increasingly used in a variety of oceanographic and naval tasks, such as oceanographic surveys, target detection and classification, and seafloor imaging. Many of these tasks make use of acoustics as either a remote sensing tool or as a communications signal carrier. Propagation of acoustic signals are highly dependent on the acoustic environment: the sea surface, water column, and sea floor. Thus, accurate understanding of this environment may be exploited for improving the performance of sonars or acoustic modems, similarly to the optimization strategies used in the past by human platform and sonar operators. Computational acoustic modeling uses numerical methods for approximately solving the wave equation in real environments whose parameters are too complex to handle analytically. This paper presents the Generic Robotic Acoustic Modeling (GRAM) concept for interfacing the artificial intelligence captaining the AUV to one or more existing acoustic models, such as the Acoustics Toolbox [1] or OASES [2] models.

The research described in this paper was funded by the Office of Naval Research under Grants N00014-08-1-0011 and N00014-08-1-0013. In addition, it was supported by the NATO Undersea Research Centre (NURC) in La Spezia, Italy, which conducted a series of joint experiments under the GOATS and GLINT Joint Research Programs, without which the current research would not have materialized.

T. Schneider and H. Schmidt are with the Center for Ocean Engineering in the Department of Mechanical Engineering, Massachusetts Institute of Technology (MIT), Cambridge, MA, 02139 USA. T. Schneider is also affiliated with the Woods Hole Oceanographic Institution (WHOI), Woods Hole, MA, 02543 USA, as a student in the MIT/WHOI Joint Program (e-mail: tes@mit.edu, henrik@mit.edu).

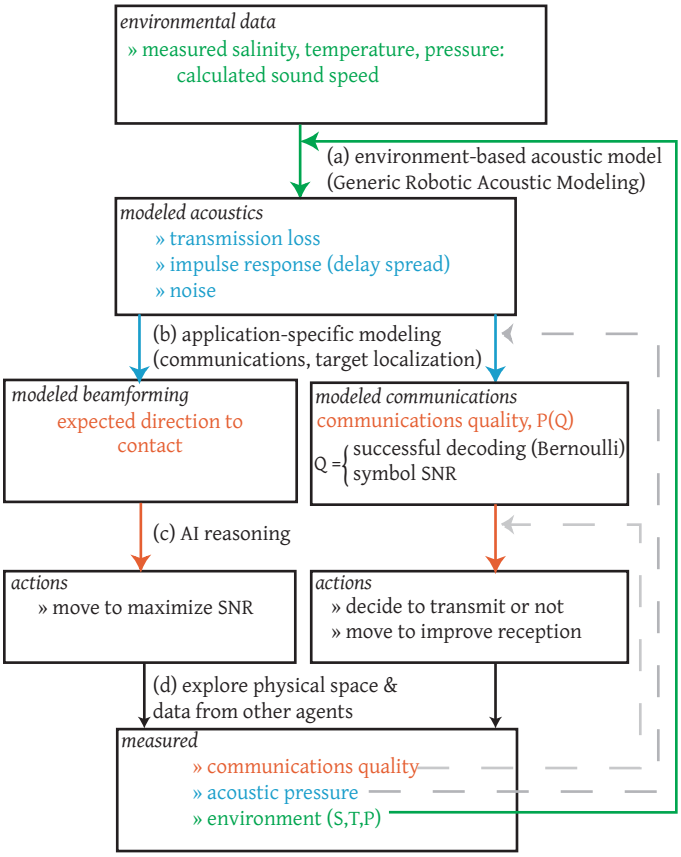

Fig. 1: Block diagram overview of the model-based adaptivity framework presented in this work. The right path focuses on improving acoustic communications (demonstrated in section III) whereas the left path models sonar performance for a target tracking application (section IV-B). Both applications (and others) can be run in parallel due to the RPC design of GRAM (see section II). The dotted arrows represent areas of feedback not presented in this work that could be exploited for better performance.

We present the use of the GRAM concept and software for two domains: improved acoustic communications in shallow water and deep sea localization and tracking of a near surface acoustic contact. A schematic of this concept is given in Fig. 1.

A. MOOS-IvP Autonomy Software

The MOOS-IvP Autonomy software presented in [3] provides two main components that form the underpinnings for this work:

- MOOS publish/subscribe middleware: provides interprocess communications (IPC) over TCP in a publish/subscribe manner via a central "bulletin-board" process which contains a database of the latest sample of each data type. This enables the robotic software to be split into many discrete subsystems that can be developed and debugged independently.
- The Interval Programming (IvP) Helm multi-objective decision engine: The IvP Helm provides an interface for a collection of behaviors to produce functions of utility (which are soft decisions and can be multi-modal) over one or more domains (usually heading, speed, and depth of the AUV). At a set frequency (typically one Hertz), the IvP Helm solves all the behaviors' functions for a single hard decision that is passed to the vehicle control system to execute. Unlike traditional behavior-based control such as that championed by Brooks [4], the IvP Helm behaviors have state and therefore can run models and act on collected data, as is done in the behaviors presented in this work.

MOOS-IvP has been used extensively in marine vehicle autonomy research, such as cooperative search tasks [5]–[7] and adaptive oceanographic sensing [8], [9].

B. Computational Acoustic Models

This work builds on several computational models that use differing techniques for approximately solving the wave equation in complex ocean environments. The theoretical treatment of the underlying approximations used for all these models is discussed in depth in [10]:

- Acoustics Toolbox: a collection of computational models and related tools. The two that are integrated into GRAM are:
  - BELLHOP [11]: a model that generates ray trajectories, transmission loss (using Gaussian beam tracing), and eigenray travel time outputs using the ray-based high-frequency approximation of acoustic propagation. This is the model used for the case studies in this work due to the rapid computation of ray tracing over other approaches. On embedded systems such as AUVs, fast computation is often more important than high fidelity due to power constraints and available computational resources. See Fig. 3 for an illustration of how much power can be saved by having a low duty cycle on the modeling system.
  - KRAKEN [12]: a normal modes based model. KRAKEN treats the ocean waveguide as a summation of modes and is thus best suited for more accurate modeling of somewhat lower frequency (fewer modes) problems than BELLHOP is suited for.
- OASES: a model that relies on wavenumber integration to solve problems involving propagation in one or more horizontally stratified layers, making it especially suited for seismo-acoustics problems.

Other acoustic models can be incorporated into the framework presented in section II. The Acoustics Toolbox and OASES were chosen for their maturity, open source availability, and performance (both are written in Fortran, which is compiled to the platform's native machine code).

II. GRAM: Low power in-situ Generalized Acoustic Modeling

The Generic Robotic Acoustic Model (GRAM) provides a set of tools implemented in C++ for performing *in-situ* modeling of the acoustic environment for use by autonomous decision making (such as the IvP Helm used in the experimental studies in sections III and IV-B). A graphical structure diagram of GRAM is provided in Fig. 2, showing also the suggested division of hardware systems based on the realtime and performance (and thereby power) requirements. GRAM is designed with several considerations that make it more suited for running on underwater embedded robotic systems than directly calling the underlying acoustic modeling code:

- asynchronous remote procedure call (RPC) design
- runtime reconfigurable
- abstracted interface

A. RPC design

GRAM is designed such that each "consumer" (an application or module that needs the result of an acoustic model) makes asynchronous requests independently of the other consumers. Each request is processed by the GRAM tools and a response is sent back containing the results of the model calculation. The requests and responses can be transmitted over a transport of choice (e.g. TCP, shared memory, RS-232); in the results presented in this paper we use the MOOS middleware TCP-based transport. This design allows for the separation of soft realtime modeling computations from other firm or hard realtime systems ("backseat" autonomous decision making and "frontseat" low-level control and actuation), as consumers can continue to work using their most recent available data until the new model calculation is complete. This separation also allows for the hardware performing the modeling to be put into a low power state, saving significant amounts of energy when the required duty cycle of the modeling farm is somewhat less than one hundred percent. See Fig. 3 for a comparison of power usage for a split model/realtime system (such as diagrammed in Fig. 2) versus a more traditional single CPU board design. The specifics of the mission and dynamics of the environment can change the required duty cycle dramatically.

B. Runtime reconfigurable

Each request for a model calculation can contain any or all of the parameters of the acoustic environment. This allows for meshing fixed parameter values with real time updates of the environment available from on-board sensors

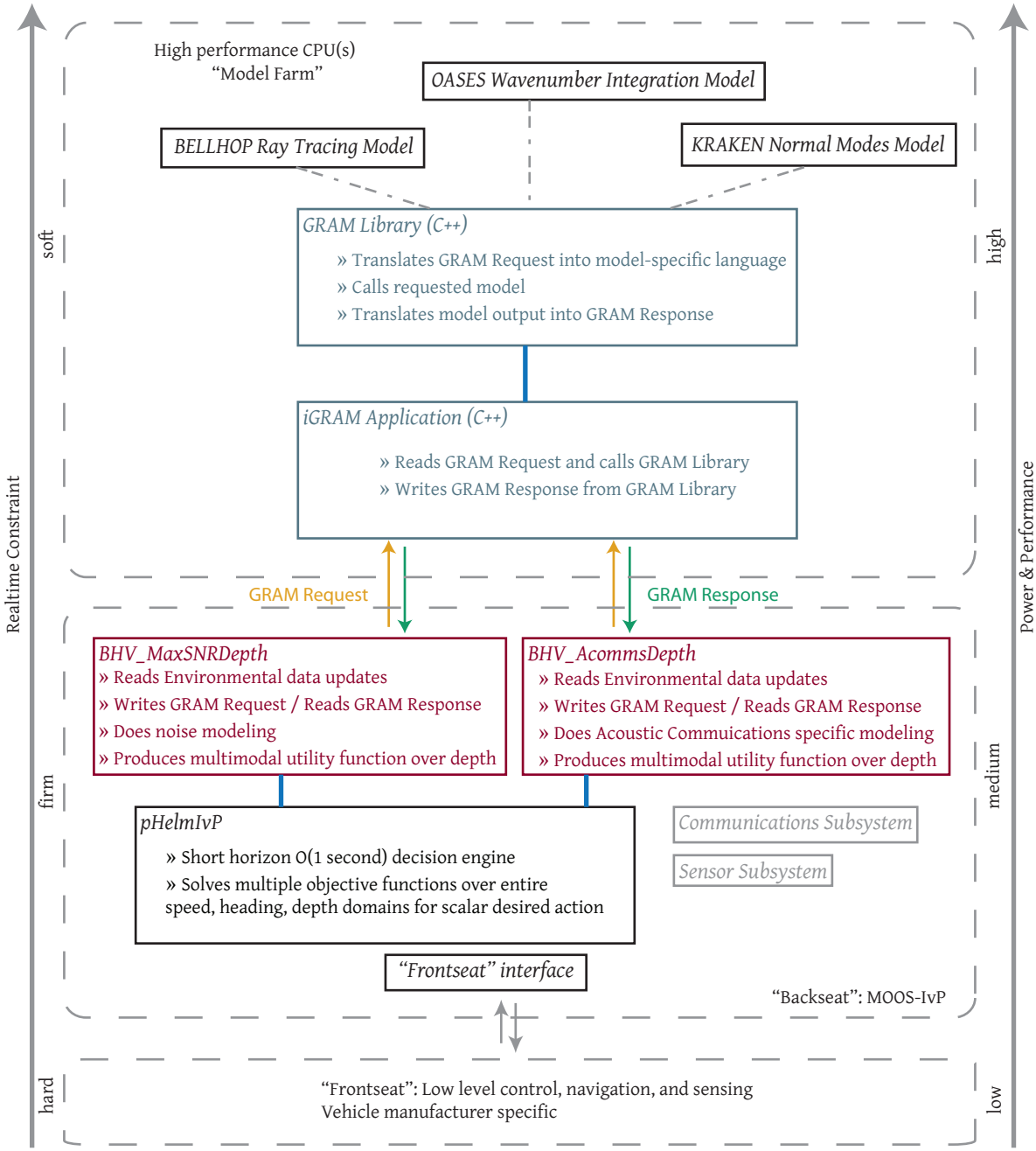

Fig. 2: A structure diagram of an autonomous underwater vehicle using the GRAM tools and the MOOS-IvP autonomy middleware. See [13] for an overview of the "frontseat"-"backseat" paradigm (Oliveira, et al. also use a similar separation of hardware in [14]). The present work adds a third physical computing layer, the model farm, which can be thought of a one step further removed in terms of realtime requirements from the "backseat". While this separation is not required, it can be used to save power, as illustrated in Fig. 3.

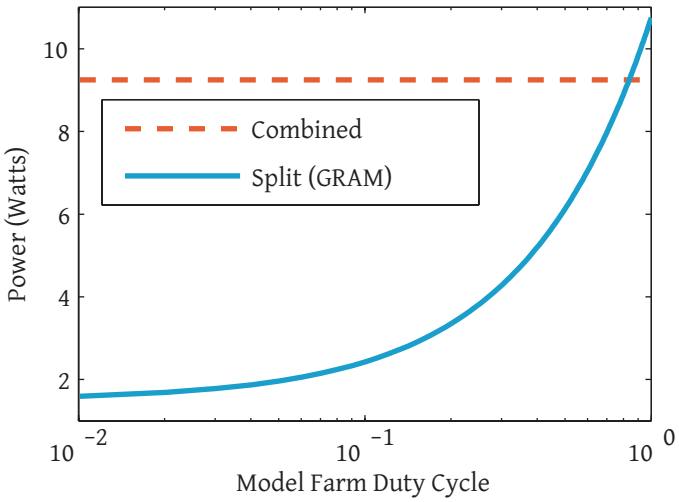

Fig. 3: Comparison of computer board power usage for *split* low-power CPU (the "backseat") and high-performance CPU ("model farm") versus *combined* on a single high-performance board. Low-power board shown is the Eurotech Titan (Intel 520 MHz PXA270 XScale processor) [15]; high-performance board is the Advantech PCM-3363 (Intel 1.8 GHz Atom D525 Dual Core processor) [16]. The duty cycle is the fraction of time the acoustic models are being run, with the assumption the model farm can be shut off in the *split* case the rest of the time. Except when the models are being run near constantly, the *split* system (illustrated in Fig. 2) saves power, which is especially useful in longer slower missions where hotel power usage dominates propulsion power usage [17].

(e.g. Conductivity-Temperature-Depth (CTD) sensor) and/or transmitted from a remote source (e.g. another AUV, satellite, surface craft).

C. Abstracted interface

GRAM uses an extensible object-oriented representation of the acoustic environment (written in a language-neutral Protocol Buffers representation [18]), which is translated into the specific input format required by the desired acoustic model. Many of these models use arcane input formats that are intolerant of syntactical mistakes. Given the costs of AUVs (hundreds of thousands of US dollars) and the operational costs of AUV experiments (thousands of dollars per day), accepted software quality practices that emphasize saving programming time and increasing reliability are of utmost concern to AUV researchers. The abstracted GRAM interfaces provides these quality checks that the native interface to the Acoustics Toolbox and OASES do not:

- compile-time type checking
- compile-time bounds checking on enumeration fields
- run-time bounds checking on numeric fields

III. GLINT10 Shallow water experiment

A. Acoustic Communications

Most autonomous vehicle tasks share a common element: collection of data that are only useful once they reach a human operator or a collaborating robot. Transmission of such data can easily be accomplished once the mission is completed and the vehicle is recovered. However, the time sensitivity of the data may preclude waiting hours or days before its recovery. Furthermore, offloading data during a mission guards against complete loss in the event of catastrophic vehicle failures. Finally, collaboration between two or more robots require communications during the mission.

To this end, wireless acoustic communication systems have been developed to allow for subsea telemetry. Sound is used as a carrier rather than the more traditional radio or light waves due to the very short electromagnetic skin depth of sea water in all but very low frequencies (which require large antennas to efficiently generate). Acoustic waves are far from an ideal digital signal carrier, though. Attenuation due to absorption which increases with frequency puts a practical upper bound on the usable carrier frequencies and consequently available bandwidth. Multipath due to surface and bottom reflections as well as refraction caused by the often highly stratified vertical sound speed profile leads to intersymbol interference and thereby high packet loss. The low speed of sound in water (nominally 1500 m/s) leads to non-negligible Doppler effects. Stojanovic [19], Preisig [20], and Baggeroer [21] cover all these issues and how they influence the design of an acoustic modem physical layer.

B. Experimental Setup

The GLINT10 experiment took place in the shallow water (nominally 110 meters deep) off Porto Santo Stefano, GR, Italy in the Tyrrhenian Sea within ten kilometers of the experiment datum at $42°27'24''$ N, $10°52'30''$ E. The acoustic environment (see Fig. 4) was marked by a warm surface layer (corresponding to a high speed of sound) followed by a sharp thermocline and cooler water. From the perspective of this work, the experiment has two goals:

1) Collect statistics on acoustic modem performance as a function of range and depth for use in validating the utility of the adaptive behaviors and for developing feedback learning for future missions. On previous experiments in a similar environment, qualitative observations had been made about much improved modem performance at deeper depths. This experiment hopes to validate and quantify this observation.
2) Demonstrate an adaptive behavior `BHV_AcommsDepth` for tracking the modeled transmission loss minimum calculated using the sound speed profile obtained by the AUV using the thermocline detection and tracking behaviors developed as part of [9].

Both of these were performed using a single AUV ("Unicorn") and a communications buoy ("Buoy") fixed at 30 meters depth. Both assets were equipped with the WHOI acoustic Micro-Modem in the "C" frequency band using modulation rate "0": see Table I for the corresponding acoustical and modulation parameters. This choice of modem hardware was driven by availability and convenience; the adaptive behaviors in this work are based on fundamental acoustics that affect

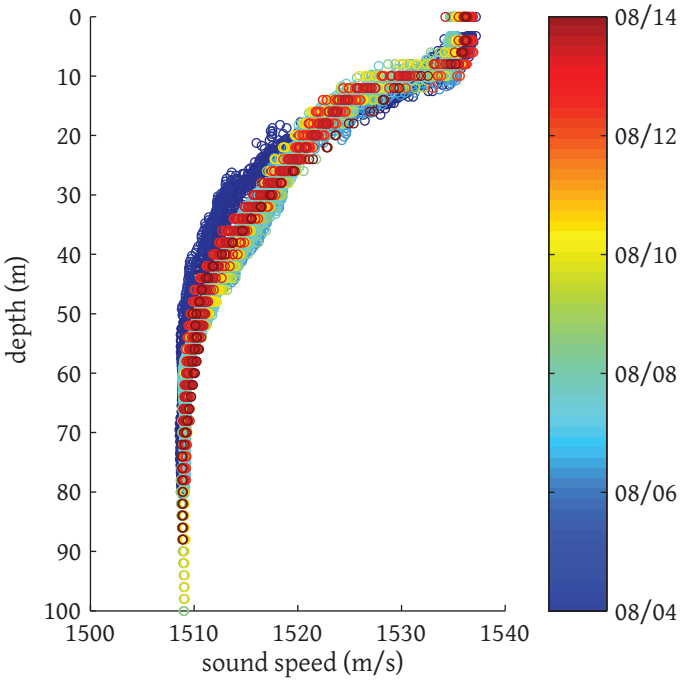

Fig. 4: The 111 sound speed profiles calculated using the Chen/Millero equation [24] from the temperature, salinity, and pressure data collected by the AUV Unicorn throughout the GLINT10 experiment starting on 4 August 2010. Profiles were collected by the AUV performing one or more "yoyo" maneuvers in depth and are averaged over thirty minute windows. Initially the stratification is more pronounced before a storm early in the experiment caused some mixing of surface and bottom waters.

TABLE I: GLINT10 Experiment Parameters

Geometric	
Source (Buoy) depth	30 m
Receiver (AUV) depth	variable (primarily 0-60 m)
Source (Buoy) speed	0.03 m/s (σ = 0.02 m/s)
Receiver (AUV) speed	1.47 m/s (σ = 0.14 m/s)
Source beam pattern	azimuthally omni-directional; polar is 5dB reduced towards surface and bottom.
Environmental	
Sea state (Beaufort)	1-3
Sea floor depth	111 m (σ = 4.7 m)
Signaling[a]	
Source Level	190 dB re 1 μPa at 1 m
Frequency (carrier)	25120 Hz
Bandwidth	4160 Hz
Modulation	Frequency-hopping Frequency Shift Keying (FH-FSK)
Frequency hops	7
Symbol bin width	320 Hz
Symbol duration	6.25 ms
Symbol clearing time	6 symbols = 37.5 ms
Error correction coding	rate 1/2 convolutional code
Symbols / transmission	576
BHV_AcommsDepth	
Acoustic model window τ_a	120 s
Environmental window τ_e	1800 s

[a] See [22] for further details on coding and modulation and [23] for the packet specification.

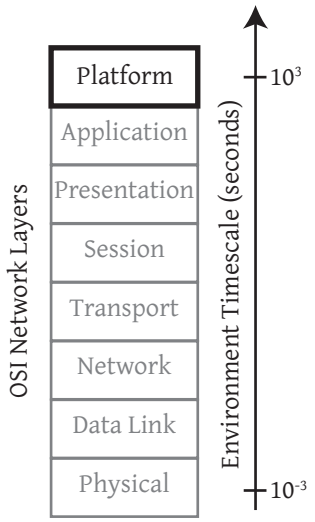

Fig. 5: The work in this section can be thought of as comprised of a new layer above the traditional seven-layer Open Systems Initiative (OSI) networking stack [25]. Another way of thinking about this compared to other work in the networking system is the timescale of environmental changes that are focused on; that is, the physical layer is concerned with symbol-to-symbol variation in the channel (milliseconds), whereas this work tackles hourly or longer scale variation in the environment.

the performance of all acoustic modems. Different modulation schemes and adaptive equalization will cause improved results in certain environments, but they cannot remedy the underlying signal's quality. The behaviors developed here work to improve the underlying signal which should in turn improve modem performance regardless of the modem chosen. This work is complementary to that on the physical layer such as [26] and [27], and operates on a level above the traditional networking "stack" in a new layer called the "platform" layer as shown in Fig. 5. The timescales involved are widely different as well: `BHV_AcommsDepth` aims to improve communications taking into account environmental changes on the order of hours whereas physical layer communications work is attempted to account for changes on the order of milliseconds.

C. BHV_AcommsDepth: Autonomy Behavior for maximizing acoustic modem performance over vehicle depth

This IvP Helm behavior was written to arbitrate over the depth decision domain with the goal of improving acoustic communications reception between an AUV and a fixed (or slowly moving) receiver. It makes use of the modeled acoustics to form a soft decision based on the expected best communications throughput.

Using the newest available sound speed data `BHV_AcommsDepth` makes a request to GRAM for a

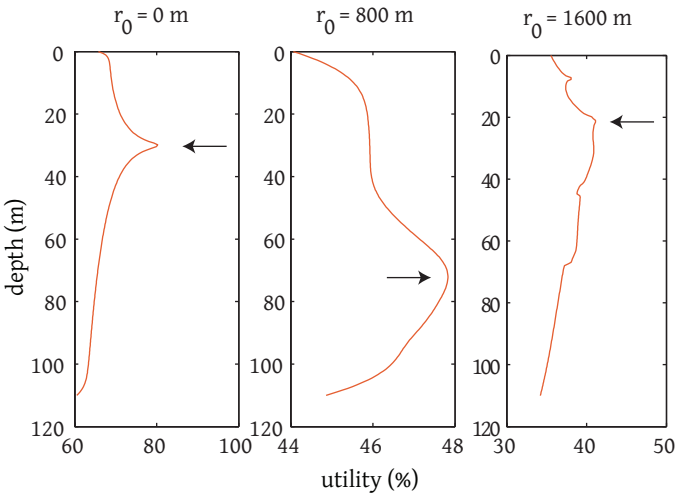

(a) Three example plots of the BHV_AcommsDepth objective function $O(d)$ (Eq. 3) using the ray trace shown in Fig. 8, Θ = 0, H_{max} = 108 dB, and remaining parameters as given in Table I. In the absence of other behaviors, the vehicle's decision for depth is marked by an arrow.

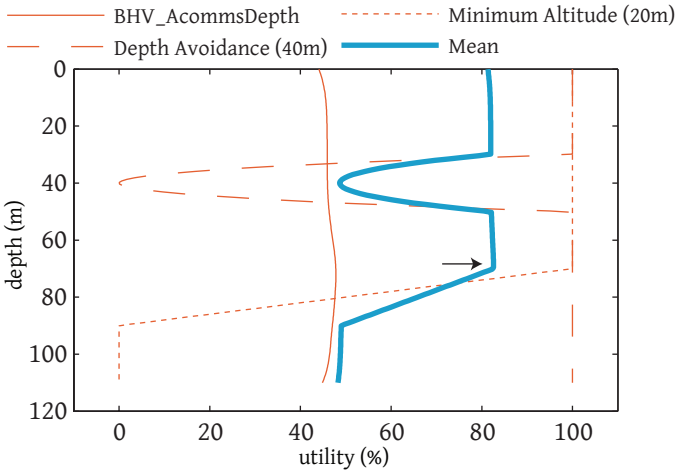

(b) One possible interaction of BHV_AcommsDepth with other behaviors. The objective function for r_0 = 800m is shown along with two other behaviors (one for avoiding a hypothetical obstacle at 40m and a safety behavior to stay 20m off the sea floor). Again, the decision is given by an arrow.

Fig. 6: Example BHV_AcommsDepth objective functions without (a) and with (b) concurrent depth-domain behaviors.

transmission loss calculation for the range window Δr where

$$\Delta r = |\vec{v}_0| cos(\Theta) \tau_a \tag{1}$$

formed from the vehicle's current position r_0 for a predefined time horizon τ_a based on its current instantaneous velocity $\vec{v}_0$ and angle Θ with respect to the Buoy (where $\Theta = 0$ is defined as when the AUV's bow is pointing directly away from the buoy's position). This request is made at least every τ_a seconds so that the modeled region in range-depth space (with respect to the receiver) always contains the actual region that the vehicle currently occupies.

The sound speed is assumed homogeneous in range (i.e. the Northings/Eastings plane) given the infeasibility of sampling all points in the vehicle's future path. `BHV_AcommsDepth` then averages the modeled intensity over the range window to calculate the modeled transmission loss

$$\overline{H(d)} = -10 \log_{10} \left(\left[\sum_{r=r_0}^{r_0+\Delta r} \left| \frac{P(d,r)}{P_0} \right|^2 \right] / \Delta r \right) \tag{2}$$

where $P(d,r)$ is the acoustic pressure in AUV depth (d) and range (r), and P_0 is the pressure at the source. Using this averaged transmission loss, `BHV_AcommsDepth` seeks to maximize the expected acoustic signal level via an objective function ($O(d)$) over AUV depth

$$O(d) = \max \left(1 - \frac{\overline{H(d)}}{H_{max}}, 0 \right) \tag{3}$$

where H_{max} is a normalization constant representing the transmission loss threshold above which the vehicle is assigned no utility to be at that depth. This can either be the maximum H for a given window (as was used in the GLINT10 trial) or a global maximum determined based on the received signal statistics. For the data collected during this experiment, a H_{max} of 108 dB would be a reasonable choice as less than 1% of messages were received at measured transmission losses higher than this. This value was used in the objective functions plotted in Fig. 6. Another more aggressive choice could be the minimum probability of error decision rule for the binary hypothesis test between a packet being received successfully or a packet being dropped. Based on the GLINT10 data, this criterion would lead to $H_{max} = 94$ dB.

The completed objective function $O(d)$ is then passed to the IvP Helm to solve along with the other behaviors for the heading and speed domains. An example of how $O(d)$ interacts with other objective functions that also operate in the depth decision domain is illustrated in Fig. 6b.

D. Mission profile

This experiment was designed to test the effectiveness of model-based adaptivity on a single AUV without expensive equipment such as an upward-facing Acoustic Doppler Current Profiler (ADCP) which could measure sea-surface conditions. The required equipment for this experiment was only a CTD and enough computational power to run the MOOS-IvP and GRAM combined autonomy and modeling system.

Each mission was run with a basic straight-line "racetrack" in the Northings/Eastings local UTM Cartesian plane. The interesting part of the mission happens in depth, with the goal that the `BHV_AcommsDepth` would run simultaneously with other behaviors arbitrating over the Northings/Eastings plane (via a chosen desired speed and heading). In addition, it is expected that other behaviors will be added to influence the chosen depth of the vehicle, and the multi-objective solver of the IvP Helm resolving these multiple functions over the vehicle's utility for a given depth. Each mission followed this plan:

1) Gather a CTD profile by making sinusoidal excursions in depth, starting with close to the full water column and narrowing down to adapt to the thermocline region where the most changes in temperature (and by extension sound speed in this environment) are occuring. This thermocline adaptivity is described in [9].

2) These CTD data are passed to `BHV_AcommsDepth` which generates an objective function for the IvP Helm to solve along with the other behaviors for the heading and speed domains. The BELLHOP model was used with GRAM for this work due to the high frequency (25 kHz) of the acoustic carrier. For this experiment, no behaviors besides `BHV_AcommsDepth` were running that produced an objective function over depth, so that we could evaluate the performance of `BHV_AcommsDepth` alone.
3) The vehicle moves to the optimal depth determined by `BHV_AcommsDepth` and at least every τ_a seconds reruns the GRAM model from step 2) taking into account changes in heading and speed. Less often (at the environmental interval τ_e) a reset to step 1) is made to remeasure the sound speed profile and for any changes in the environment. τ_e should be much less than the timescale of changes to the environment. Since the shallow water Mediterranean sound speed profile changes significantly on the order of one day timescales, τ_e was chosen to about a two orders of magnitude below that, or 1800 seconds.

E. Results

1) Modeling and communications statistics: The modeling and statistical results of the GLINT10 experiment are summarized in Fig. 7. Fig. 7 (a) shows a BELLHOP ray tracing model for the average sound speed profile of the entire experiment to give a general overview of the acoustic environment from the perspective of the Buoy as source and show the significant downward refraction due to the thermocline from 10 to 30 meters depth. Note that this average erases some of the small scale features present in each actual profile (taken every τ_e seconds and plotted in Fig. 4) that the vehicle actually uses for its modeling.

For display purposes, the remaining plots are split into 400 meter range bins where all data shown within are averaged in range over these bins. Only the upper 60 meters of the water column are shown as this is where the AUV spent most of its time. Fig. 7 (b) gives the modeled transmission loss ($H_n(d)$) using the profiles (instantiations) taken by the vehicle and then averaged in intensity over the instantiations as well as within each range bin, that is

$$H_n(d) = -10\log_{10}\left(\frac{1}{i_{max}}\sum_{i=0}^{i_{max}} 10^{-H(d,i)/10}\right) \qquad (4)$$

where $H(d,i)$ is given by equation 2 for each instantiation of the sound speed profile i. In this case $\Delta r = 400$ and $r_0 = \Delta r(n-1)$ where $n = [1,5]$ corresponds to each of the five displayed range bins. The error bars (standard deviation of the intensity over all the sound speed profile instantiations) show the sensitivity of various parts of the transmission loss plot to changes in the sound speed profile. The regions of higher standard deviation are caused by caustics moving location due to small changes in the sound speed profile. In general, deeper depths have lower H in this environment.

Fig. 7 (c) gives the modeled root-mean-square delay spread τ_{RMS} calculated using the experiment mean sound speed profile (SSP) (Fig. 7 (a)) where

$$\tau_{RMS} = \sqrt{\frac{\int_0^\infty (\tau-\bar{\tau})^2 A(\tau)d\tau}{\int_0^\infty A(\tau)d\tau}} \qquad (5)$$

and $A(\tau)$ is the intensity of the arrivals where $\tau = 0$ is the first arrival. In general, deeper water has a lower delay spread, leading to potentially reduced intersymbol interference.

The experimental data from all the transmissions ($N = 3350$) sent by the AUV Unicorn to the Buoy were used to compare against the modeled data. The data were split into two groups using a basic division interesting to AUV roboticists: was the message received correctly (R=good) or not (R=bad)? A message was considered to be received correctly if it had no errors after decoding (as verified by a cyclic redundancy check in the WHOI Micro-Modem). Any other problem with the message meant that it was considered not to be received correctly. A probability distribution of the vehicle's depth ($P(D)$) throughout the experiment was estimated from the data using an Epanechnikov kernel smoothing estimate. Also a conditional probability of depth given that the messages were received ($P(D|R = good)$) was computed in a similar manner. Of greater interest is the posterior probability ($P(R = good|D = d)$) which was computed for all depths d using the prior $P(D)$ and Bayes' rule:

$$P(R = good|D = d) = \frac{P(D = d|R = good)P(R = good)}{P(D = d)} \qquad (6)$$

This posterior was plotted in Fig. 7 (d). For ranges greater than 800 meters (range bins 3-5), the data show a strong depth dependency, with modem performance doubling from twenty meters to fifty meters in the farthest range bin. At short ranges ($r < 800$ m), large percentages ($P(R = good|D = depth) > 0.75$) of the messages are received which is likely due to the strong direct arrival (first bottom bounce occurs at $r \simeq 1100$ meters) and generally high signal strength. As would be expected given that modem performance depends on signal strength, this is the inverse of the modeled transmission loss in Fig. 7(b), which shows a depth dependency in the same bins (decreasing H with increasing depth). These data also do not show a strong correlation with the modeled delay spread τ_{RMS}. This may be due to the fact that the real delay spread is significantly influenced by the sea surface, which was naively modeled using a flat pressure release surface in this work due to the lack of onboard knowledge about the sea state. Furthermore, the symbol clearing time of the FH-FSK modulation employed is 37.5 ms, significantly longer than the delay spreads modeled here (the root-mean-square values are in the 10-20 ms range).

2) AUV Adaptivity: Fig. 8 shows the position of the AUV during its missions running `BHV_AcommsDepth` on 8 August 2010 overlaid with a single representative transmission loss ray trace from that day. The vehicle tracks the modeled downbeaming from 400-1000 meters well and also picks up the convergence zone off the first bottom bounce from 1400-2000 meters. As can be seen from the sensitivity analysis in

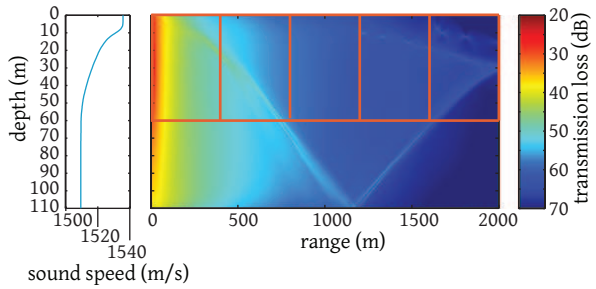

(a) Mean sound speed profile (left) used to compute representative transmission loss model (right). Boxes represent regions plotted in parts (b), (c), and (d) of this figure.

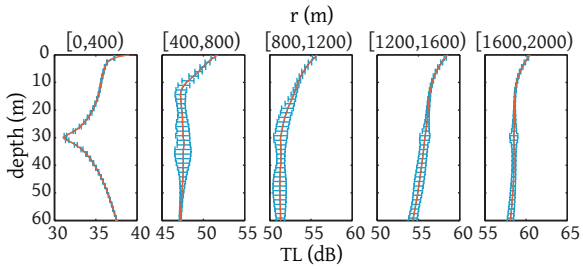

(b) Mean modeled transmission loss (H) for five range bins (each bin representing 4.4 minutes (τ_a) of averaging for a vehicle moving at 1.5 m/s.) The error bars represent the standard deviation σ for the H computed using all the sound speed profiles collected and displayed in Fig. 4.

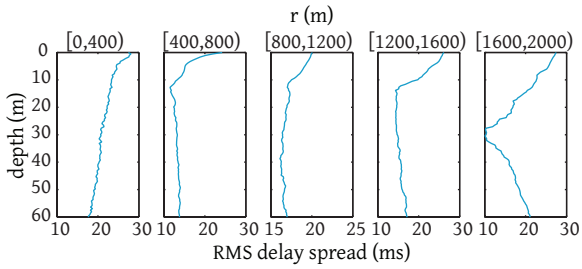

(c) Modeled root-mean-square delay spread from the mean sound speed profile shown in part (a). Due to the 37.5 ms of clearing time used by the incoherent FH-FSK modulation of the modem, we expect that this delay spread will have little effect on the successful receipt of datagrams.

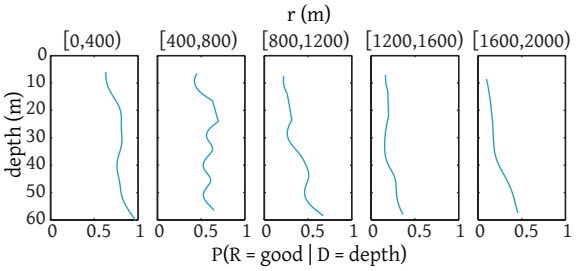

(d) Estimated conditional probability of successful receipt (R=good) plotted over the conditioning depth. Depths where the AUV was present less than 1% of the transmissions are excluded.

Fig. 7: Modeled (using GRAM and BELLHOP) and measured data from the GLINT10 experiment. Note that at longer ranges ($r > 800$ m), there is a inverse correlation between the modeled transmission loss (b) and the estimated probability of successful receipt (d), as expected.

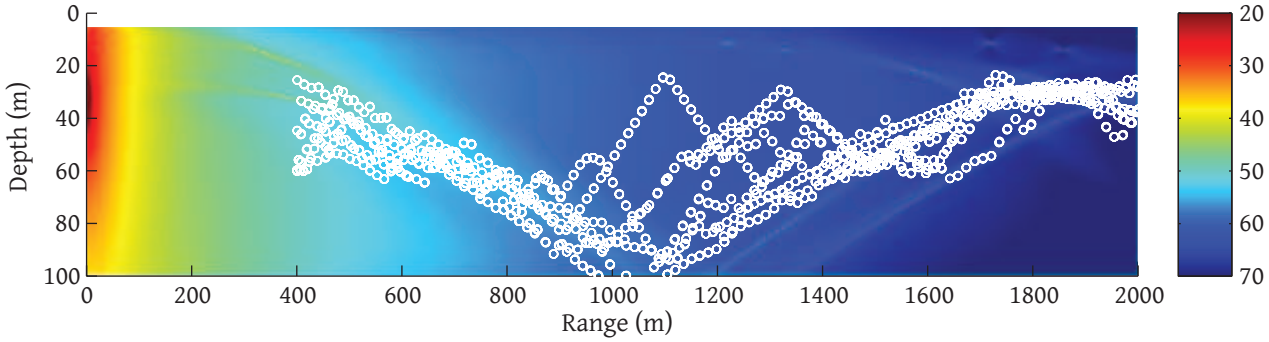

Fig. 8: Depth position of the AUV Unicorn (white circles) with respect to range from the Buoy overlaid on a representative ray trace from 8 August 2010 08:28:19 Z.

Fig. 7(b), the region from 800-1200 has the highest sensitivity to changes in the sound speed profile. The AUV is responding to modeled caustics in this region that may or may not be real and are unlikely to be where they are predicted to be due to differences in the real environment from the model. This suggests an area of improvement for `BHV_AcommsDepth` to filter its objective function with a low pass filter with a cutoff inversely proportional to the measured sensitivity. By doing so, the `BHV_AcommsDepth` would make less certain choices in light of uncertainty, leaving depth decisions up to behaviors that have more knowledge.

IV. Acoustic Connectivity in Deep Ocean Environments

In contrast to littoral environments, the bulk of the deep ocean is well isolated from atmospheric forcing, reducing the temporal variability on hourly and daily scale to a small fraction of volume close to the surface. Thus, the features of sound speed profile most significant to the acoustic environment are extremely stable, most notably the isothermal gradient dominating the sound speed profile below the SOFAR channel, controlling the dominant convergence zone propagation characteristic of deep ocean acoustics.

Another feature of the deep ocean which makes depth

adaptation beneficial is the strong spatial diversity of the ambient noise. Thus, in shallow water, the ambient noise field tends to be dominated by the local, surface-generated noise. The noise from distant shipping and atmospheric disturbances will undergo significant attenuation due to the strong bottom interaction inherent to shallow water propagation. In contrast, the upward-refracting deep sea sound speed gradient allows noise from distant, natural and man-made sources of ambient noise to be carried over long distances with limited or no bottom interaction [10]. In very deep ocean environments in particular, this can result in an ambient noise field which is highly depth dependent. Thus, at depths above the critical depth, the ambient noise field has significant contributions from both local surface sources, and distant shipping and storms. Below the critical depth the acoustic field due to distant sources is evanescent, and the noise field is reduced to that produced by sources within a horizontal range of approximately half a convergence zone, the so-called Reliable Acoustic Path (RAP) cone. Consequently a reduction in noise of several dB can be expected near the bottom in such environments, which may be exploited by the platform autonomy.

Another feature associated with the interplay of signal and noise which may be exploited is the spatial diversity of the array gain. Thus, the performance of the acoustic array processing not only depends on the signal-to-noise ratio (SNR), but also on the angular distribution of the signal and noise components. For a deep receiver platform communicating with a shallow collaborator, the most reliable acoustic path will follow the convergence zone path, and the dominant elevation angle at the deep node will depend on the range: positive for short ranges, and negative for ranges beyond half a convergence zone (approx. 30 km). Similarly, the noise directionality will depend on the horizontal source distribution, potentially leading to a strong depth dependence of the array gain which may be exploited for optimal system performance.

These features of the signal to noise trade-offs are conveniently captured in the classical *sonar equation*, which may be modeled by the GRAM infrastructure in combination with environmental information provided to the undersea platforms via the command and control infrastructure.

A. Depth Adaptation for Sonar Equation Optimization

In its simplest form the *Passive Sonar Equation* relevant to passive acoustic sensing and to underwater communication takes the form [10]

$$\mathrm{SE} = \mathrm{SL} - \mathrm{H} - \mathrm{NL} + \mathrm{AG}, \tag{7}$$

where SE is the resulting *signal excess*, SL is the *source level*, H the *transmission loss*, NL the *noise level* and AG is the *array gain*, all expressed in dB.

Figure 9 illustrates how an optimization of the system performance can be straightforwardly achieved in the MOOS-IvP autonomy architecture expanded by the GRAM environmental acoustic modeling framework.

The *Mission Manager* processes are responsible for maintaining the situational awareness of the autonomy system. To generate the current *environmental picture* including sound speed profile, noise profiles, and noise directionality, dedicated MOOS processes are fusing environmental information from all available sources, including i) historical data in on board databases; ii) environmental updates received from the *Field Control* via the acoustic communication network; iii) in-situ measurements by environmental sensors; and iv) on-board modeling.

The current environmental estimates resulting from this data fusion are assumed to be slowly varying and are therefore stored in the MOOSDB for use by the modeling infrastructure and the autonomy behaviors. For example, the overall depth-dependence of the SSP, and the noise level NG and array gain AG, will rarely be available from in-situ local measurements, and will therefore be fixed at mission start. On the other hand, occasional updates of the near-surface SSP, the location of local shipping traffic, and local noise measurements may be used to update the environmental picture, which is then published in the appropriate MOOS variables, allowing the platform to adapt to changes in the ambient noise field etc. For example the OASES model can be used through GRAM to estimate the current noise directionality, which may subsequently be used to update the estimate of the array gain for the current geometrical configuration.

In addition, the *Mission Manager* is maintaining the *situational awareness*, including navigation information for the platform itself, collaborating platforms, and acoustic contacts, required for the acoustic modeling of the transmission loss, and keeps track of the current geometry of receiving acoustic arrays and sources on-board the platform, which is required for the array gain term in the sonar equation.

Based on the currently available *environmental and situational picture* the autonomy system can generate objective functions which optimize the sonar equation (Eq. 7), or components thereof. For that purpose a dedicated MOOS-IvP behavior, `BHV_MaxSNRDepth` has been developed. Thus, as illustrated in Fig. 9, it will first retrieve the depth-dependence of the ambient noise NL from the MOOSDB. Then, it will submit a request to iGRAM for a current estimate of all ray arrivals predicted for the acoustic contact of interest. Using a local plane-wave representation the behavior it will continuously use this ray expansion to generate an estimate of the current array response, representing the terms $AG - H$ in the sonar equation. This performance metric is shown in the lower, center plot as contours versus elevation angle and depth in the water column. The behavior then combines the two depth-functions into one depth objective function, representing the utility versus depth for the sensing objective. As described earlier, this objective function is then merged with other depth behavior objective functions by the IvP multi-objective optimization algorithm.

The reason for choosing variable weighting of the signal and noise components in the sonar equation is the fact that their reliability can vary significantly. Thus, the average historical ambient noise profile may have a significant uncertainty, in particular in regions with heavy seasonal shipping or atmospheric conditions. In such cases the weight of the NL terms should be reduced. Similarly, if the propagation environment is highly variable, more weight may be applied to the noise

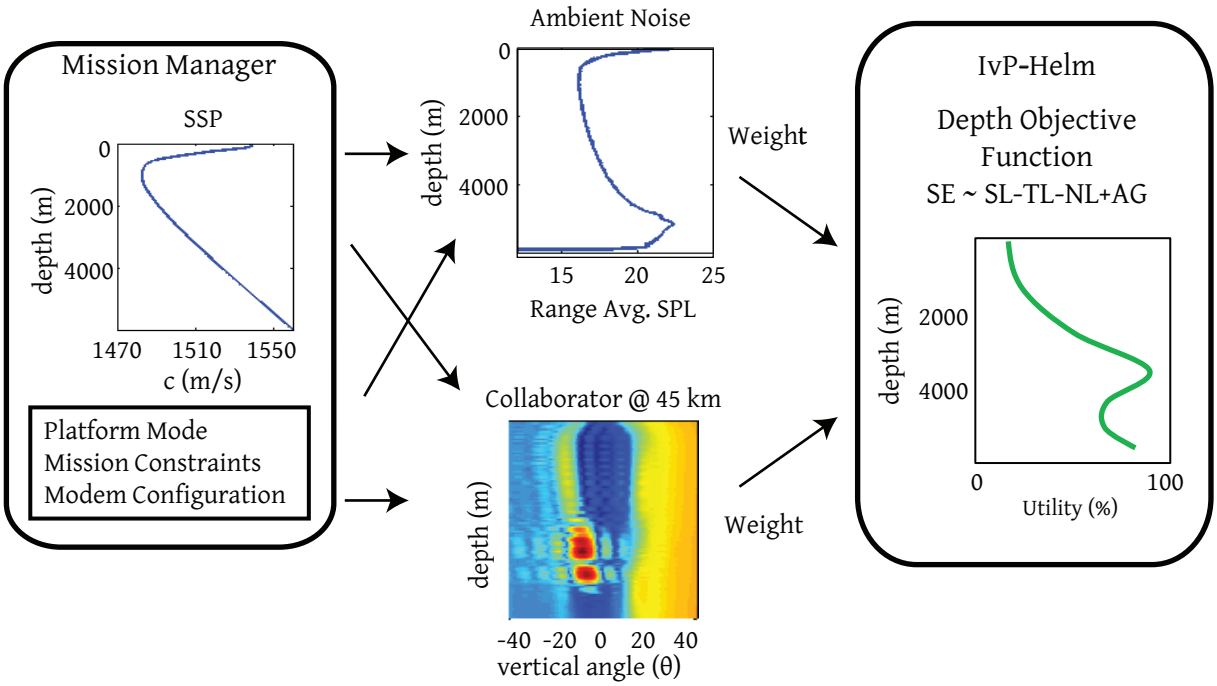

Fig. 9: Functionality of model-based depth adaptation on a deep submersible for minimizing signal-noise ratio for maintaining optimal acoustic connectivity with near-surface acoustic contact. The on-board mission manager process will, based on the current environmental and situational information, request from GRAM a forecast of the estimated transmission loss. This forecast is then combined with estimates of the other terms in the sonar equation for planning the future depth trajectory, thus improving connectivity.

profile in choosing the optimal depth.

Although the principle of the depth-adaptation as described above is rather simple, there are a couple of subtle issues associated with the use of the concept in deep water.

The first is the nature of the caustics characteristic to the deep convergence zone propagation. As described earlier, caustics also play an important role for depth-adaptation in shallow water. However, the convergence zone caustics associated with a deep source or receiver can be modeled with high confidence level due to the extraordinarily stable nature of the deep sea SSP gradient. Further, in contrast to the shallow water case, the convergence zone caustics of relevance to deep platforms always have the shadow zone above the caustic. Therefore, robustness requires that a bias towards depth be built into the depth objective function. Parameter studies have shown that for realistic variations of the near surface SSP and realistic depth uncertainty of the acoustic contact, the depth of the caustic can be predicted with an error of order 50 m. Hence, a low-pass filtering of the raw depth-objective function with a spatial cutoff frequency of 1/50 m^{-1} , starting at the surface, will yield an optimal depth of order 100 m below the predicted caustic, well into the 'safe zone'.

Another issue of particular importance to the deep water application is the time scales associated with depth changes. The maximum pitch of an AUV is of order $20°$, which for a typical platform speed of 1.5 m/s yields a maximum rate of depth change of 0.75 m/s. Hence, it takes more than 20 minutes required to change the depth by 1 km. In contrast, an AUV operating in 100 m deep shallow water can reach any new depth in less than a couple of minutes. Consequently, the forecasting horizon required for the adaptive depth change will have to be significantly larger. On the other hand, the decision to change depth cannot be based on a fixed forecasting horizon. For example, to reach a certain depth in 30 minutes may require that the platform cross through a shadow zone, which is obviously detrimental to the acoustic connectivity. Thus, decisions about depth changes have to be made on the basis of the entire time from the present to the chosen maximum time horizon. In `BHV_MaxSNRDepth` this is done by forecasting the depth objective function over a set of ranges up to and including the forecasting horizon. Then, the depth decision is made based on the following, simple, strategy:

- If the platform is already at or near the optimal depth locally, it will remain there by choosing a short time forecast as a basis for the adaptation.
- If the local depth is not any longer near the optimal, e.g. when approaching a range where a convergence zone caustic is forming, the behavior will select as a target depth the optimal depth at a range within the forecast horizon, which can be reached with the minimum platform pitch.

The first criteria will ensure that once the platform has reached a stable optimum, it will track it until a discretely different optimum starts developing somewhere in the section of the water column allowed for the adaptation. The second criteria will ensure that the platform is not forced to change depth

so fast that it crosses into a shadow zone to reach a future optimum. In other words, the platform will try to reach an optimum depth 'ridge' tangentially. Of course this is all assuming that the contact motion continues at the current range rate and heading. Also, the depth control is not made in pitch directly, but in depth, so whenever significant depth changes are requested, the platform will increase the pitch to maximum. However, since this process is repeated at the rate of the IvP Helm updates, typically of order of a second, the depth adaptation will occur smoothly, as illustrated in the simulation example following.

B. Deep Sea Simulation Example

For demonstrating the deep ocean performance of the acoustic connectivity optimization behavior, we will use the high-fidelity simulation environment developed and established at MIT. This virtual environment provides a virtual ocean environment with high-fidelity simulation of the environmental acoustics, using the GRAM embedded modeling infrastructure. In addition to the environmental acoustic modeling, the simulator also incorporates hydrodynamic models of both the submersible and sonar arrays, as well as the ability to simulate the supporting acoustic communication networking. The fidelity of the simulation environment allows the testing of the exact same autonomy software and configuration as applied in actual field deployments.

To illustrate the performance of the MOOS-IvP behavior `BHV_MaxSNRDepth` in adapting to the local acoustic environment, we consider as an example the autonomous acoustic connectivity of a deep submersible in a Pacific environment with a water depth of 6000 m, with a critical depth of 4000 m. The submersible is tasked to maintain acoustic connectivity with an acoustic contact at 200 m depth, opening range at a rate of 5 m/s (10 kn). The ambient noise is assumed to be constant to the critical depth, and then decay linearly by 3 dB/km towards the bottom. The submersible is initially deployed at 5000 m depth, performing a hexagonal loiter pattern of radius 500 m. No particular array geometry is considered, and the depth adaptaion simply optimizes the signal-to-noise ratio.

When the contact range exceeds 15 km, the `BHV_MaxSNRDepth` behavior is activated and determines that a caustic, and associated optimal depth exists at a depth of 3000 m. The behavior in this case is configured to forecast 2 hours into the future, and determines that it can reach the caustic at a range of 30 km and a depth of 4000 m and initiates the depth change since it is not currently at an optimum depth. Because of range estimation uncertainty and the fact that the behavior uses a conservative contact range estimate, the submersible reaches the caustic at a range of 23 km, after which the adaptation strategy will make it track the optimal depth below the caustic, as evidenced by the actual track shown in the figure by white circles. Note that the apparent depth rate of the submersible does not appear constant during the ascent. This is due to the loiter of the submersible, leading to variations in the range rate. When the range exceeds 40 km, the maximum pitch of the submersible does not allow it to continue to track the caustic, and it instead continues to climb at its maximum pitch.

To illustrate the performance of the low-pass filtering of the depth objective function, Fig. 11 shows the raw depth objective function at 43 km range for the example in Fig. 10. The left plot shows the raw depth objective function for minimizing the signal-to-noise ratio, while the right plot shows the low-passed filtered objective function with a maximum 100 m below the depth of the convergence zone caustic.

V. Conclusion

In this work, the new Generic Robotic Acoustic Modeling (GRAM) tool was introduced for successfully utilizing existing acoustic models on embedded processors onboard autonomous underwater vehicles. GRAM was applied to two representative problems: improving communication in an anisotropic shallow water environment, and maintaining contact with an acoustic target in the deep sea.

In addition to the examples given here, GRAM has applicability for software-only simulation of actual sonars as well as hardware-in-the-loop testing of modem systems (where signals from an existing hardware modem are delayed and convolved with the channel measured by GRAM). These tools are available as part of the open source LAMSS project (https://launchpad.net/lamss) and access is available upon request to the authors.

Acknowledgment

We thank Michael Porter for the Acoustics Toolbox models and the WHOI Micro-Modem group led by Lee Freitag for their assistance with their acoustic modem.

A particular thanks to the staff and collaborators at NURC, and the crew of NRV Alliance and CRV Leonardo, the expertise and seagoing capability of which is unmatched anywhere in the world.

References

[1] M. B. Porter, "The acoustics toolbox." [Online]. Available: http://oalib.hlsresearch.com/Modes/AcousticsToolbox/

[2] H. Schmidt, "Oases: Ocean acoustic and seismic exploration synthesis." [Online]. Available: http://lamss.mit.edu/lamss/pmwiki/pmwiki.php?n=Site.Oases

[3] M. R. Benjamin, H. Schmidt, P. M. Newman, and J. J. Leonard, "Nested Autonomy for Unmanned Marine Vehicles with MOOS-IvP," *Journal of Field Robotics*, vol. 27, no. 6, pp. 834–875, November/December 2010.

[4] R. Brooks, "Intelligence without reason," *Artificial intelligence: critical concepts*, vol. 3, 1991.

[5] A. Shafer, "Autonomous cooperation of heterogeneous platforms for sea-based search tasks," Master's thesis, Massachusetts Institute of Technology, 2008.

[6] T. Schneider, H. Schmidt, T. Pastore, and M. Benjamin, "Cooperative autonomy for contact investigation," in *OCEANS 2010 IEEE-Sydney*. IEEE.

[7] D. Hughes, S. Kemna, M. Hamilton, and R. Been, "Sensible behaviour strategies for auvs in asw scenarios," in *OCEANS 2010 IEEE-Sydney*. IEEE, 2010.

[8] D. Eickstedt, M. Benjamin, H. Schmidt, and J. Leonard, "Adaptive control of heterogeneous marine sensor platforms in an autonomous sensor network," in *Intelligent Robots and Systems, 2006 IEEE/RSJ International Conference on*. IEEE, 2006, pp. 5514–5521.

[9] S. Petillo, A. Balasuriya, and H. Schmidt, "Autonomous adaptive environmental assessment and feature tracking via autonomous underwater vehicles," in *OCEANS 2010 IEEE-Sydney*. IEEE.

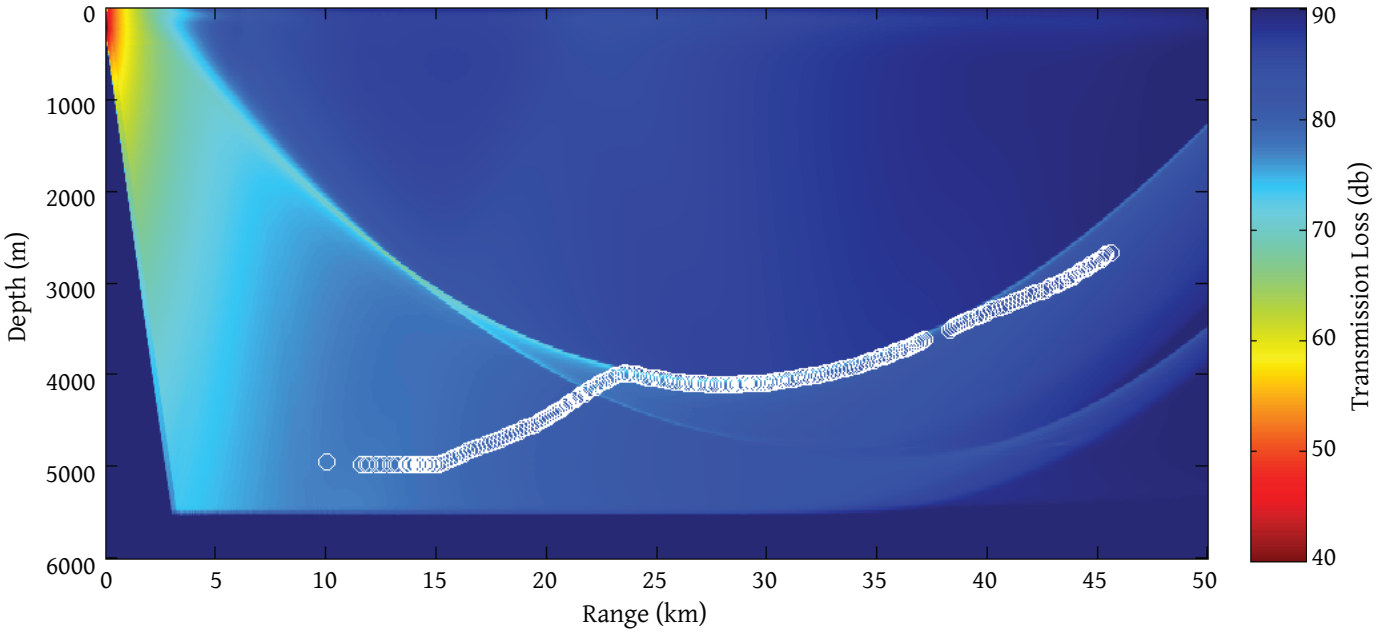

Fig. 10: Contours of transmission loss in dB for a moving acoustic source at 200 m depth in deep water environment, plotted vs depth and the range from from the source. White markers show the adaptive path of a deep submersible optimizing acoustic connectivity with surface source, constrained by a maximum pitch of 20 degrees.

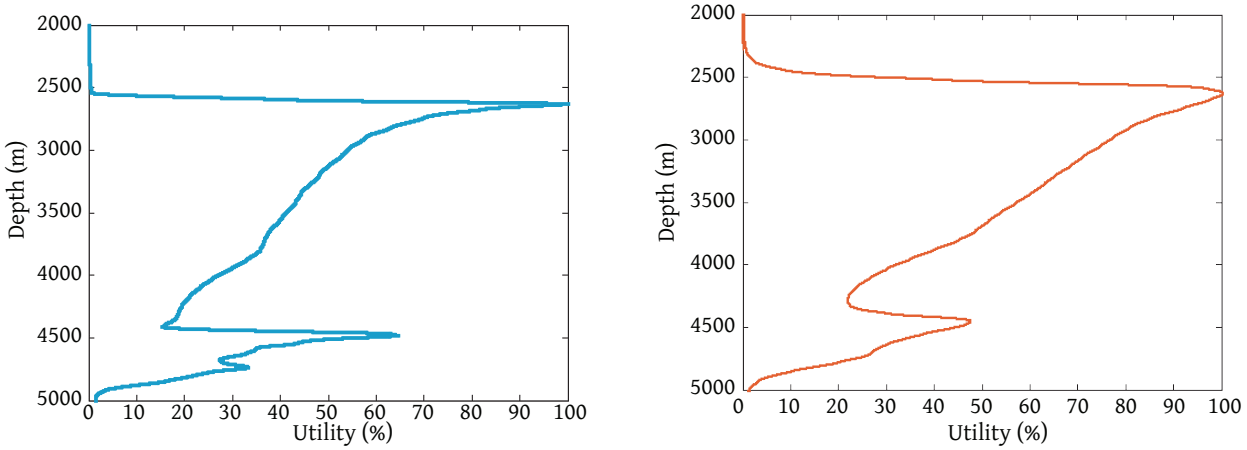

(a) Raw objective function showing sharp caustic at 2500 m depth.

(b) Low-pass filtered corresponding to depth-uncertainty of caustic of 50 m.

Fig. 11: Forecasted depth objective function at 43 km range.

[10] F. Jensen, W. Kuperman, M. Porter, and H. Schmidt, *Computational ocean acoustics*. Springer London, Limited, 2011.

[11] M. Porter and Y. Liu, "Finite-element ray tracing," in *Proc. Int. Conf. on Theoretical Comp. Acoust*, vol. 2, pp. 947–956.

[12] M. B. Porter, "The KRAKEN normal mode program," SACLANT Undersea Research Centre, Tech. Rep., May 2001. [Online]. Available: http://oalib.hlsresearch.com/Modes/kraken.pdf

[13] T. Schneider and H. Schmidt, "Unified command and control for heterogeneous marine sensing networks," *Journal of Field Robotics*, vol. 27, no. 6, pp. 876–889, 2010. [Online]. Available: http://dx.doi.org/10.1002/rob.20346

[14] P. Oliveira, A. Pascoal, V. Silva, and C. Silvestre, "Mission control of the marius auv: System design, implementation, and sea trials," *International journal of systems science*, vol. 29, no. 10, pp. 1065–1080, 1998.

[15] *Titan PXA270 RISC based PC/104 Single Board Computer Technical Manual*, EuroTech, Ltd. [Online]. Available: http://www.eurotech.com/en/pb.aspx?tab=download&pg=titan

[16] *User Manual: PCM-3363*, Advantech Co., Ltd.

[17] A. Bradley, M. Feezor, H. Singh, and F. Yates Sorrell, "Power systems for autonomous underwater vehicles," *Oceanic Engineering, IEEE Journal of*, vol. 26, no. 4, pp. 526–538, 2001.

[18] Google, "Protocol buffers: Developer guide." [Online]. Available: http://code.google.com/apis/protocolbuffers/docs/overview.html

[19] M. Stojanovic, "Underwater acoustic communications: Design considerations on the physical layer," in *Wireless on Demand Network Systems and Services, 2008. WONS 2008. Fifth Annual Conference on*. IEEE, 2008.

[20] J. Preisig, "Acoustic propagation considerations for underwater acoustic communications network development," *ACM SIGMOBILE Mobile Computing and Communications Review*, vol. 11, no. 4, 2007.

[21] A. Baggeroer, "Acoustic telemetry–An overview," *IEEE J. Ocean. Eng.*, vol. 9, no. 4, pp. 229–235, 1984.

[22] L. Freitag, "Fhfsk coding and modulation specification," Woods Hole

Oceanographic Institution, Tech. Rep. 401003-SPEC, 2005. [Online]. Available: http://acomms.whoi.edu/publications/

[23] L. Freitag and S. Singh, "Compact data layer for acoustic communications," Woods Hole Oceanographic Institution, Tech. Rep. 401002-SPEC, 2004. [Online]. Available: http://acomms.whoi.edu/publications/

[24] C. Chen and F. Millero, "Speed of sound in seawater at high pressures," *J. Acoust. Soc. Am*, vol. 62, no. 5, pp. 1129–1135, 1977.

[25] International Telecommunication Union, "Information technology - open systems interconnection - basic reference model: The basic model," Internation Telecommunication Union, Tech. Rep. X.200, 1994.

[26] W. Li and J. Preisig, "Estimation of rapidly time-varying sparse channels," *Oceanic Engineering, IEEE Journal of*, vol. 32, no. 4, pp. 927–939, 2007.

[27] L. Freitag, M. Stojanovic, S. Singh, and M. Johnson, "Analysis of channel effects on direct-sequence and frequency-hopped spread-spectrum acoustic communication," *Oceanic Engineering, IEEE Journal of*, vol. 26, no. 4, pp. 586–593, 2001.

Toby Schneider (M'05) received a B.A. in physics at Williams College in Williamstown, MA, USA in 2007.

He is currently a graduate student working towards a Ph.D. in ocean engineering in the Joint Program in Oceanography/Applied Ocean Science and Engineering between the Massachusetts Institute of Technology in Cambridge, MA, USA and the Woods Hole Oceanographic Institution in Woods Hole, MA, USA (http://mit.whoi.edu/).

Mr. Schneider is also a member of the Acoustical Society of America. Further professional details about Mr. Schneider are available on his website: http://gobysoft.org.

Henrik Schmidt is Professor of Mechanical & Ocean Engineering at the Massachusetts Institute of Technology. He received his MS degree from The Technical University of Denmark in 1974, and his Ph.D. from the same institution in 1978. Following a post-doctoral fellowship at the Risoe National Laboratory in Denmark, he joined the NATO Undersea Research Centre in Italy in 1982, where he worked until he joined the MIT faculty in 1987. Professor Schmidt's research has focused on underwater acoustic propagation and signal processing, and most recently on the development of environmentally adaptive acoustic sensing concepts for networks of autonomous underwater vehicles. Prof. Schmidt is a Fellow of the Acoustical Society of America, and he is the 2005 recepient of the ASA *Pioneers of Underwater Acoustics Medal*